

Loughborough University Institutional Repository

Physical vapour deposition of thin films for use in superconducting RF cavities

This item was submitted to Loughborough University's Institutional Repository by the/an author.

Citation: WILDE, S. ... et al, 2015. Physical vapour deposition of thin films for use in superconducting RF cavities. IN: Proceedings of the 6th International Particle Accelerator Conference IPAC2015, 3rd-8th May 2015, Richmond, Virginia, USA. JACoW, pp. 3249 - 3252.

Additional Information:

- This is a conference paper published by JACoW and distributed under the terms of the Creative Commons Attribution 3.0 license (CC-BY 3.0).

Metadata Record: <https://dspace.lboro.ac.uk/2134/19514>

Version: Published

Publisher: JACoW

Rights: This work is made available according to the conditions of the Creative Commons Attribution 3.0 Unported (CC BY 3.0) licence. Full details of this licence are available at: <http://creativecommons.org/licenses/by/3.0/>

Please cite the published version.

PHYSICAL VAPOUR DEPOSITION OF THIN FILMS FOR USE IN SUPERCONDUCTING RF CAVITIES

S. Wilde^{1,3}, R. Valizadeh¹, O.B. Malyshev¹, G. B. G. Stenning², A. Hannah¹, D.O. Malyshev¹, S. Pattalwar¹, B. Chesca³

¹ASTeC, STFC Daresbury Laboratory, Warrington, UK

²ISIS, STFC Rutherford Appleton Laboratory, Didcot, UK

³Department of Physics, Loughborough University, Loughborough, UK

Abstract

The production of superconducting coatings for radio frequency cavities is a rapidly developing field that should ultimately lead to acceleration gradients greater than those obtained by bulk Nb RF cavities. Optimizing superconducting properties of Nb thin-films is therefore essential. Nb films were deposited by magnetron sputtering in pulsed DC mode onto Si (100) and MgO (100) substrates and also by high impulse magnetron sputtering (HiPIMS) onto Si (100), MgO (100) and polycrystalline Cu. The films were characterised using scanning electron microscopy, x-ray diffraction and DC SQUID magnetometry.

INTRODUCTION

Superconducting radio frequency (SRF) cavity technology in particle accelerators is now reaching the limit of performance achievable with bulk Nb cavities [1]. Since superconducting properties for SRF are confined to a penetration depth of less than one micron [2] then Nb thin-films offer an alternative to bulk Nb with the advantage of Cu substrates which have a factor of three higher thermal conductivity than Nb [3]. A Nb thin-film which is oriented parallel to a magnetic field can have a higher first critical magnetic field than bulk Nb if the film is thinner than the London penetration depth. There is also the possibility of multilayer films that provide greater magnetic shielding [4]. With better thermal stability and higher critical fields it is possible to have higher accelerating gradients within SRF cavities allowing for better performance, reduced cost and reduced volumes of Nb [5]. Physical vapour deposition by magnetron sputtering has been used as a preferred process due to its high deposition rate and ease of scalability in order to produce superconducting thin films within SRF cavities [6,7]. The purpose of the present study is to compare films deposited by both pulsed DC and HiPIMS and to compare films deposited onto Si (100), MgO (100) and polycrystalline Cu substrates. Nb thin films were deposited using the Advanced Energy Pinnacle + in pulsed DC mode. Films were then deposited by HiPIMS using an Ionautics HiPSTER 1000 power supply. HiPIMS has a characteristic peak current which is two orders of magnitude higher than pulsed DC at the expense of a reduction in deposition rate. The variable parameters are deposition current, voltage, pulsed duty cycle, pulsed frequency, substrate temperature, and substrate bias. After

morphological evaluation the films have then been assessed for their superconducting properties showing their suitability for use in SRF cavities.

EXPERIMENTAL

Thin film samples were deposited simultaneously onto Si (100), MgO (100) and polycrystalline Cu substrates using Kr sputtering gas. Each substrate was prepared by cleaning in ultrasonic baths of acetone, methanol, IPA, then deionised water [8]. In the case of HiPIMS deposition, the substrate was then plasma cleaned using oxygen plasma, then ion bombarded for 30 minutes before deposition. The pulsed DC power was set to 400 W at 350 kHz with a 50% duty cycle. The HiPIMS power supply was varied between 100 and 400 W. Pulse lengths were operated between 100 and 300 μ s at frequencies between 100 and 300 Hz. A typical current – voltage – time profile for the HiPIMS power supply is shown in Fig 1.

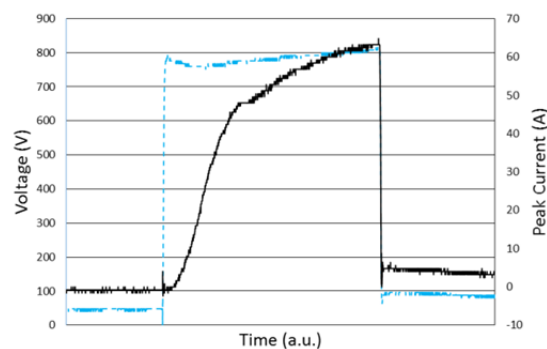


Figure 1: The current – voltage – time profile of a HiPIMS pulse. Peak current is shown in black and voltage in blue.

The current voltage characteristics of both power supplies are shown together in Fig 2. A DC bias voltage can be applied to the substrate and was varied between 0 and -100 V. RF biasing was used at 19 W. The base pressure of the unbaked UHV chamber reached $\sim 10^{-8}$ mbar and the Kr pressure was set to 3 mbar.

Morphological analysis was performed by SEM and XRD. SEM analysis was used to determine the film structure and grain size at the surface. XRD analysis results show average grain size and lattice orientations within the film. RRR measurements have been performed using a purpose built cryostat housing a four point probe.

DC SQUID magnetic susceptibility measurements were performed using a Quantum Design MPMS, giving both the first and second critical fields, H_{C1} and H_{C2} .

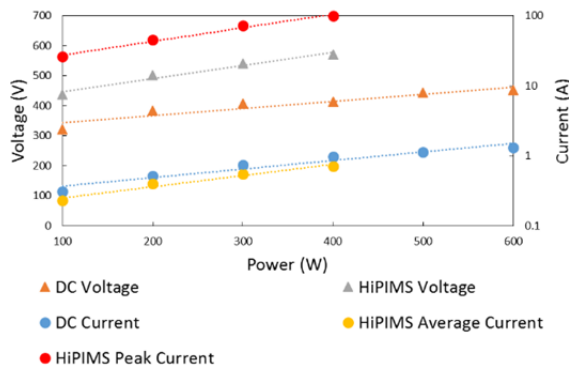


Figure 2: Current - voltage characteristics of both the pulsed DC and HiPIMS power supplies.

RESULTS AND DISCUSSION

XRD analysis has been used to compare grain size and orientation of deposited films.

Figures 3 and 4 show comparable depositions onto MgO substrate by pulsed DC and HiPIMS. Each deposition was performed at 330 °C with 400 W power and with a -100 V biased substrate. HiPIMS was set to 300 Hz repetition rate and 100 μ s pulse length. Average grain size increases from 26 nm for pulsed DC to 73 nm for HiPIMS. The same HiPIMS deposition onto polycrystalline Cu substrate resulted in Nb (110) grains of 24 nm and a smaller peak corresponding to the Nb (200) orientation (Fig 5).

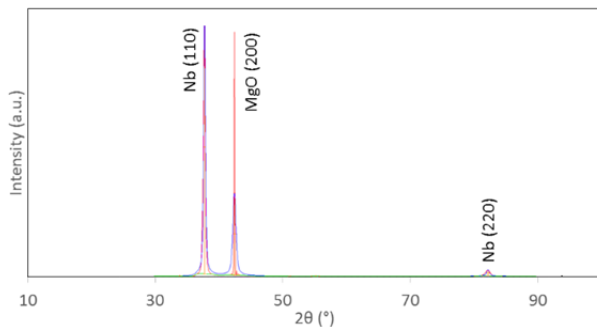


Figure 3: Nb (110) grown on MgO by pulsed DC with -100 V DC bias. Average grain size is 26 nm.

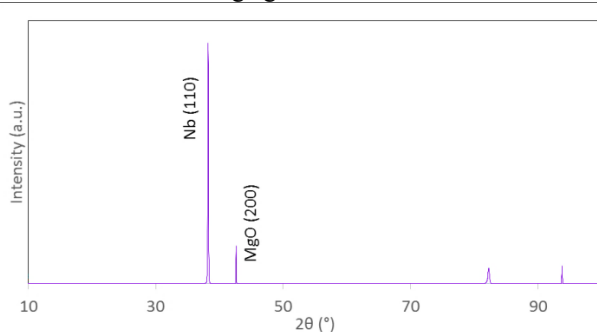


Figure 4: Nb (110) grown on MgO by HiPIMS with -100 V DC bias. Average grain size is 73 nm.

Other HiPIMS depositions onto Cu resulted in average grain sizes of 16 to 27 nm. Average grain size on MgO was seen to increase with a 19 W RF bias relative to -100 V DC bias for pulsed DC sputtering with grains up to 36 nm. Films deposited by pulsed DC onto Si (100) substrate formed with average grain size of no larger than 18 nm [7].

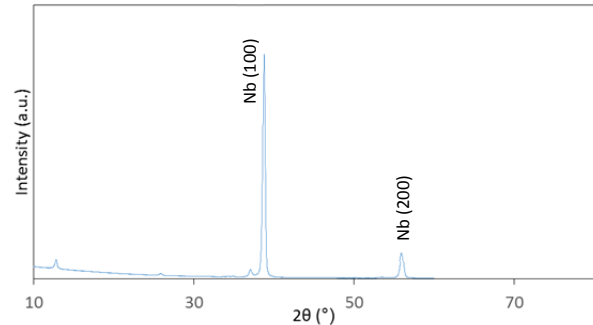


Figure 5: Nb (110) and (200) grown on polycrystalline Cu by HiPIMS with -100 V DC bias. Average grain size is 24 nm.

Residual resistivity ratio (RRR) is used to compare the quality of deposited films. High RRR is assumed to be a more uniform film with fewer electron scattering centres and therefore lower numbers of defects. RRR was compared on both Si (100) and polycrystalline Cu substrate and the values are shown in table 1. As Si, Cu and MgO substrate grown samples were deposited simultaneously in the same plasma then differences in RRR can be attributed only to substrate type. RRR values are highest in all cases for the same deposition onto Cu relative to Si (100). It was found that in all cases the RRR was highest for polycrystalline Cu substrate where RRR approximately doubled. The increasing RRR is due to better matching of the lattice parameters for Nb/Cu than for Nb/Si [9]. Nb/MgO samples have not yet been measured by RRR.

DC SQUID magnetic susceptibility measurements were performed at a temperature of 6 K on films A, B and C (Table 1) deposited by HiPIMS. Each sample was aligned such that its surface was parallel to the applied magnetic field. The value of H_{C1} is determined as the point where the magnetic field begins penetrating into the sample and is required to be at least as large as the 1800 Oe of bulk Nb. The value of H_{C2} is defined as the point where the magnetic field suppresses superconductivity completely [10]. Film C deposited onto both Si (100) and polycrystalline Cu is compared by DC SQUID measurements in Figs 6 and 7.

There is a notable difference in the shape of the hysteresis curves in each measurement. Figure 6 shows film C deposited onto Si (100) that has very unstable flux pinning in the sample. Vortices in the sample move with a viscous motion into the most stable pinning locations as the magnetic field applied to the sample changes. It can be seen at the highest magnetic fields that the momentum of the shifting vortices is so high that it causes the

Table 1: Differing RRR Values for Samples Deposited by HiPIMS onto Si (100) and Polycrystalline Cu

| Film | Power (W) | Temp (°C) | Pulse Width (µs) | Repetition Rate (Hz) | DC Bia (-V) | Peak Current (A) | Si RRR | Cu RRR |
|------|-----------|-----------|------------------|----------------------|-------------|------------------|--------|--------|
| A | 400 | 330 | 100 | 300 | 100 | 26 | 19 | 30 |
| B | 300 | 330 | 100 | 200 | 100 | 27 | 12 | 23 |
| C | 300 | 330 | 150 | 100 | 100 | 37 | 13 | 27 |

magnetic moment to change sign just before superconductivity is extinguished at H_{C2} .

Figure 7 shows film C deposited onto polycrystalline Cu. H_{C2} in this case drops from 5000 Oe for the Si (100) substrate to 3205 Oe therefore showing less flux pinning for the Cu substrate. Less flux pinning can be linked to increasing RRR for Cu substrate as the volume of imperfections in the sample must be diminished. Flux pinning for Nb / Cu is also more stable with less magnetisation jumps and therefore less fluid motion of vortices. H_{C1} does not vary greatly for either substrate.

H_{C2} of films A and B was highest for Nb/Si compared to Nb/Cu. There were fewer flux jumps therefore less fluid motion and consequently more stable flux pinning in every sample deposited onto polycrystalline Cu when compared to its Si counterpart. H_{C1} was compared for all films measured and there seemed to be no correlation between substrate or RRR. H_{C1} values above 1500 Oe were measured for both Si and Cu substrates and for RRR ranging between 19 and 27. Film B deposited onto polycrystalline Cu had the highest H_{C1} value recorded from all samples at 1846 Oe (Fig 8).

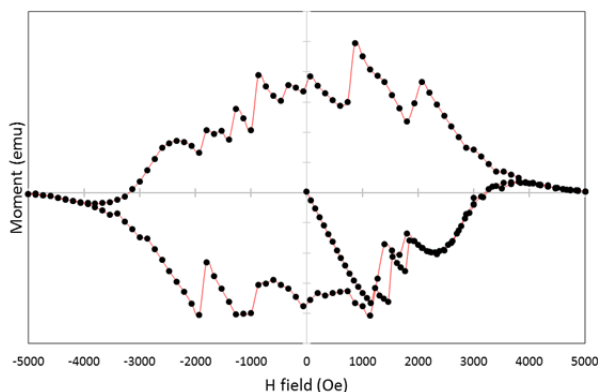


Figure 6: Magnetic hysteresis loop $M(H)$ for film C deposited onto Si (100). $H_{C1} = 1153$ Oe and $H_{C2} = 5000$ Oe.

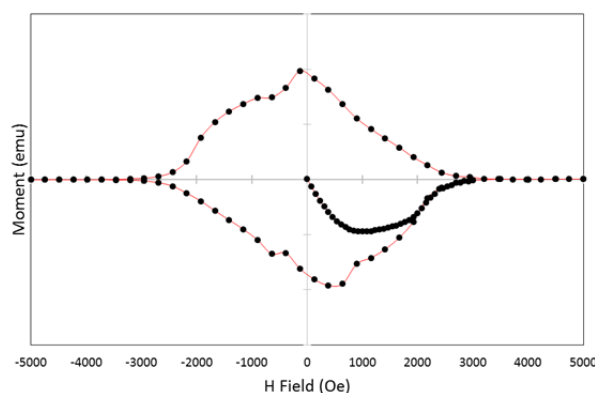


Figure 7: Magnetic hysteresis loop $M(H)$ for film C deposited onto polycrystalline Cu. $H_{C1} = 1076$ Oe and $H_{C2} = 3205$ Oe.

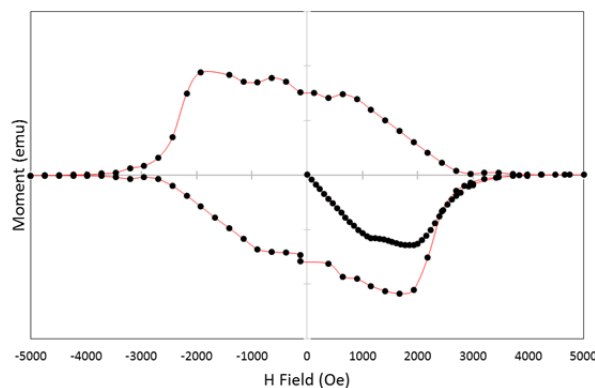


Figure 8: Magnetic hysteresis loop $M(H)$ for film B deposited onto polycrystalline Cu. $H_{C1} = 1846$ Oe and $H_{C2} = 3827$ Oe.

CONCLUSIONS

HiPIMS films deposited onto MgO (100) showed larger average grain size when correlated to comparable pulsed DC films increasing from 26 nm Nb (110) for pulsed DC to 73 nm Nb (110) for HiPIMS. Average grain size for HiPIMS films on polycrystalline Cu ranged 16 – 26 nm. RRR was seen to approximately double for samples deposited onto polycrystalline Cu when compared to the same deposition onto Si (100). DC magnetisation measurements showed less flux pinning in films deposited onto polycrystalline Cu when compared to the same deposition on Si (100) resulting in lower H_{C2} on Cu. No correlation was found between RRR or choice of Cu or Si substrate on H_{C1} however values above 1800 Oe of bulk Nb were recorded.

REFERENCES

- [1] P. Kneisel et al., Proc of PAC-2005, p. 3991 (2005).
- [2] W. Roach et al., PRST-AB 15, 062002 (2012).
- [3] C. James et al., IEEE Trans. Appl. Supercond. 23, 3500205 (2013).
- [4] A. Gurevich. Appl. Phys. Lett. 88, 012511 (2006).
- [5] C. Antoine, "Thin film technologies for SRF," EUCARD2 WP12.2 (2014).
- [6] C. Benvenuti et al., Physica C: Supercond. 316, 153 (1999).
- [7] S. Wilde et al., Proc. of IPAC'14, p. 2406 (2014).
- [8] D. Beringer and C. Reece, Proc. of SRF-2011, p. 883 (2011).
- [9] C. Benvenuti et al., 10th Workshop on RF superconductivity, p 252 (2001).
- [10] W. Buckel and R. Kleiner, Superconductivity: fundamentals and applications, (Germany: WILEY-VCH, 2004).